Thermodynamic study of methane multilayers adsorbed on graphite

Jeffrey J. Hamilton and David L. Goodstein
California Institute of Technology, Mail Code 63-37, Pasadena, California 91125
(Received 18 March 1983)

We have made thermodynamic measurements of the properties of methane adsorbed on graphite in the ranges, roughly, 1—6 molecular layers and 64—105 K. Interpreting the results in the context of current models, we tentatively conclude that layer by layer, critical points occur at approximately constant temperature around 78 K. Extrapolation of this observation would imply a roughening transition in bulk solid methane at about that temperature. We also observe a line of melting transitions that extends from the bulk triple point, $T_t = 90.7$ K, into the multilayer region at nearly constant temperature. The transition in films of less than ~ 5 layers does not appear to be first order, but it is associated with a change in entropy. The change in entropy gradually diminishes, vanishing entirely at about 2 layers. It is not clear how the transition closes, but a number of possibilities is discussed.

I. INTRODUCTION

There has been a very considerable recent surge of interest in multilayer adsorbed films.[1-9] This interest has, however, centered on the solutions of theoretical models, with only very little reference to experiment. In this paper we present a new experimental survey of a relevant multilayer system, methane on graphite.

The graphite substrate has become the industry standard for large surface area studies of adsorption because of its homogeneity and reproducibility. In this study we have chosen to use exfoliated graphite foam. Methane is a convenient adsorbate for a number of reasons. The temperatures and pressures of interest are easily accessible; both limiting cases, the monolayer and the bulk, have been studied extensively by a variety of techniques, and the same variety of techniques will ultimately be available to supplement the data of our study of multilayer films. We have used the thermodynamic technique (combining heat-capacity and vapor-pressure data) to survey the methane on graphite system between, roughly, 1 and 6 layers, and between 64 K (below the presumed gas-liquid critical point in the first layer) and 105 K (above the triple point of the bulk).

The theoretical expectations for how various multilayer systems might behave are sufficiently complex that little progress can be made without first having a broad overview of the behavior of a particular system. For that reason, we have made our measurements on a preset grid of coverages and temperatures. Having completed that survey, we set forth in this paper tentative conclusions so that they may be on record for future testing by independent data. Our strategy may be better appreciated after a brief review of the theoretical situation.

The most comprehensive of the theoretical studies has been by Pandit, Schick, and Wortis[1] (PSW), based on solutions of a lattice-gas model suggested by de Oliveira and Griffiths.[2] We shall adopt their nomenclature as a context within which to discuss our results. In PSW's scheme, the nature of the system is governed by three temperatures on the bulk coexistence curve: the wetting temperature T_W, the roughening temperature T_R, and the critical point T_C.

At all temperatures above T_W (which may be 0 K) complete wetting occurs. That means the film grows smoothly with increasing chemical potential, from zero coverage all the way to the bulk. We see no evidence of any other kind of behavior in our system; T_W for methane on graphite appears to be below 64 K. This observation is a useful first step in reducing the multiplicity of behaviors the model has prepared us to search for. Moreover, $T_C = 190.6$ K for methane, far above the temperatures of interest here.

The theoretical prediction that is most relevant to our work concerns the meaning of what experimentalists usually call a stepwise-adsorption isotherm. An example from our own data is shown in Fig. 1. Before the recent flurry of theoretical interest, data of this kind were merely taken to mean a substrate sufficiently uniform that layers formed distinctly. Crudely, one would expect steps in lower layers as long as the difference in binding energy between layers was larger than $k_B T$, with the steps becoming smeared at higher coverages.

In PSW, however, steps are evidence of gas-liquid condensation in each layer. The gas-liquid coexistence in the nth layer has a critical temperature $T_c(n)$, and this series of critical temperatures approaches a limiting value as $n \to \infty$. In the original model of de Oliveira and Griffiths, $T_c(\infty)$ is just the bulk T_c. However, since their calculations omitted the effects of the roughening transition, they argued that when these are properly included, then $T_c(\infty)$ should be T_R. Subsequent calculations by others[5-8] support this conclusion. In each layer, the step ceases to be vertical when $T > T_c(n)$. Since it is possible (indeed, expected) that, e.g., $T_c(2) > T_c(1)$, an adsorption isotherm between these temperatures might well show a smeared first step with sharp, vertical subsequent steps. We discuss below the practical difficulties in assessing experimental data for this kind of behavior.[10]

We know of no evidence (prior to this work) of a

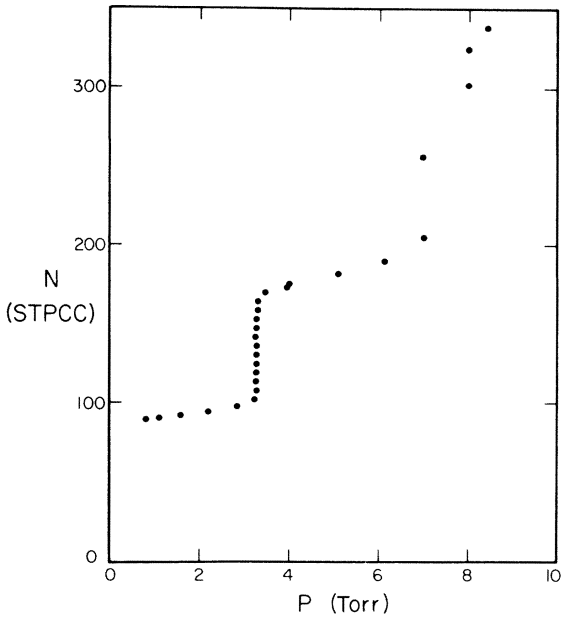

FIG. 1. Methane-film vapor-pressure isotherm at 77.4 K. At this temperature the saturated bulk vapor pressure, P_0 is 9.53 Torr.

roughening transition in bulk solid methane.[11] Thus, T_R, which plays an important role in the theory, has no clear experimental counterpart. On the other hand, methane does have a triple point, $T_t = 90.7$ K, at which the bulk phase melts and becomes liquid. The model system does not have a triple point because the simple lattice gas PSW consider has only a single condensed phase. These differences between the theoretical and experimental systems raise a number of particularly interesting questions.

The gas-liquid interface (i.e., bulk coexistence at $T > T_t$) is intrinsically rough owing to long-wavelength capillary waves. Thus, if the bulk solid does not have a $T_R < T_t$, the triple point may simply stand in for, or preempt the roughening transition. However, T_t does not seem to be a suitable endpoint for the series $T_c(n)$ since melting and layer critical points are essentially different kinds of transitions. The question then is, how do these two phase transitions interact?

The tentative conclusion we put forth here is that in the methane-on-graphite system $T_c(n) \approx 78$ K independent of n. This implies that there is indeed a roughening transition for bulk solid methane at about the same temperature, that is, $T_R < T_t$. However, even if that supposition is correct, we are still left with an important question concerning T_t and the melting transition.

Although PSW give little guidance, except in broad qualitative terms, about how melting occurs in multilayer films, certain points are very clear. If there is a line of melting transitions extending from the bulk triple point into the thin-film region, that line must close (e.g., end on another phase boundary) because there cannot be any thermodynamic path from bulk solid to bulk liquid that does not pass through a phase transition. Moreover, melting in multilayer films is a particularly interesting phenomenon because there has been much recent theoretical progress towards understanding melting in two dimensions (2D),[12] but there is little understanding of melting in three dimensions (3D). The multilayer film is an obvious candidate for an intermediate case between two and three dimensions.

We shall present evidence that there is a line of melting transitions that extends at roughly constant temperature equal to T_t from the bulk down to about 2 layers. The transition in the film does not appear to be first order, but it is associated with a change in entropy which gradually diminishes to zero as the film becomes thinner. For comparison, 3D melting is always first order, and 2D melting is believed at least in some cases to involve only essential singularities in the thermodynamic functions. We are not able to reach any firm conclusion concerning how (or indeed, whether) the multilayer melting transition closes. It may, for example, end on just such a thermodynamically undetectable transition.

In Sec. II of this paper we outline our experimental methods. Section III states our tentative conclusions and discusses the evidence supporting them, and the situation is summarized in Sec. IV. We have chosen as much as possible in this paper to base our arguments on directly observable data. A detailed thermodynamic analysis of the data will appear elsewhere.[13]

II. EXPERIMENTAL APPARATUS AND TECHNIQUE

An adiabatic calorimeter cryostat was constructed as shown in Fig. 2. The heart of the cryostat is a cylindrical aluminum cell, filled with the substrate material, in which both heat-capacity and vapor-pressure measurements can be made. Aluminum was chosen over the more traditional material, copper, because of the cell's relatively high internal dead volume (80.4 cm^3). This dead volume was in turn made necessary by the more open structure of Grafoil foam compared to regular Grafoil. Because of aluminum's low-heat capacity per unit volume, the fin-

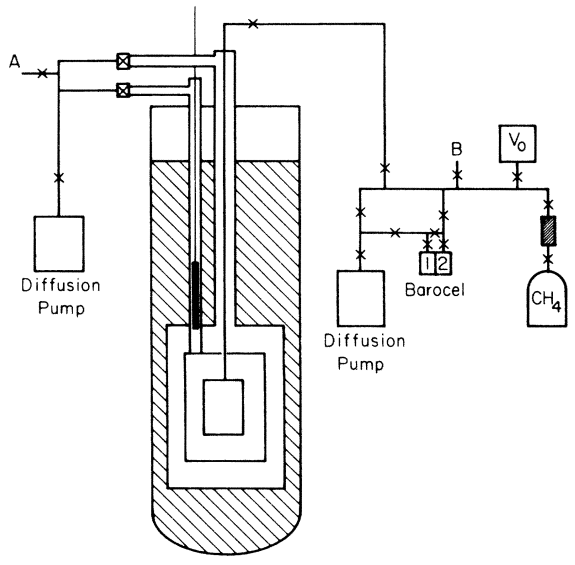

FIG. 2. Schematic diagram of the experimental apparatus.

ished cell presented an acceptable background heat capacity while remaining strong and rigid. A copper cell of the same dead volume and thermal mass would have been prohibitively fragile.

The cell is 3 cm in diameter and 10 cm high, and the cap is joined to the main body by miniature screws which also act to compress an indium *O*-ring seal. (Aluminum cannot be soldered in the way copper can.) The fill line, a 1-mm diameter stainless-steel tube, was attached to the cell cap by force-fitting it through a hole and applying stycast epoxy to both sides of the joint. This arrangement proved to be leak tight under all conditions to which it was subjected.

Before being put into the cell, the Grafoil was baked at 800 °C for a number of hours in a vacuum chamber. The sections of foam were then cut into round pieces and press fit into the cell to insure good thermal contact. At this point a stiff wire was used to poke holes through the foam, running the length of the cell, in order to facilitate the distribution of gas molecules throughout the regions of dead volume. Finally, the cell's cap was joined to the main body. In its completed form the cell consisted of 20 g of aluminum, 13 g of graphite, and 1 g of other materials.

Heater wires and thermometers were installed in the usual manner (except that Duco Cement had to be used rather than the traditional GE 7031 varnish to bond wires to aluminum), and a heater wire also ran the length of the filling line to prevent solid plugs of adsorbate from forming within it. All temperatures in this study were measured with a platinum resistance thermometer calibrated against a Lake Shore Cryotronics diode sensor, the measurements being made via a four-terminal ac Kelvin bridge.[14]

As can be seen in Fig. 2, the cell is entirely surrounded inside the vacuum space by an adiabatic radiation shield. This shield, also made of aluminum, has its own heater-thermometer combination so that its temperature can be independently monitored and adjusted relative to the cell's. Typically, in a heat-capacity run, the shield's temperature was never more than 1 K different from the cell's. Also connected to the shield is a mechanical heat switch.[15]

Helium-exchange gas can be admitted into the vacuum space via port *A*, and when not needed it can be pumped away by a diffusion pump. Meanwhile, the gas-handling part of the apparatus—completely independent from the vacuum jacket circuitry—includes its own diffusion pump, a two-liter calibrated volume, a Barocel capacitive manometer from Datametrics Inc., and the cell itself. A tank containing research-grade methane from Airco Industrial Gases forms a permanent part of this gas-handling system. The methane is 99.992% pure, and passes through an Airco No. 982P molecular filter to remove any residual traces of oxygen or water vapor. Other gases of interest can be admitted through port *B*. The diffusion pump, of course, acts to evacuate the entire system, as well as to provide a reference vacuum to chamber 1 of the Barocel. The residual pressure of this vacuum is in the low 10^{-6}-Torr range, well below one-tenth of the least significant digit read out by the Barocel on its most sensitive scale.

Vapor pressures were measured in chamber 2 of the Barocel, and a thermomolecular correction was applied according to the formula of Takaishi and Sensui[16] to determine the pressure in the cold parts of the apparatus. (Most of the time, however, this correction was insignificant.) Moreover the accuracy of the Barocel is such that the number of molecules added to the cell in any given shot can be known to better than 0.1%—a figure which arises from our uncertainty in the value of the calibrated volume. In order to prevent pressure gradients from developing within the cell (a common problem in Grafoil experiments) any time molecules were admitted to or removed from the cell the temperature was raised until the pressure was high enough to guarantee that the molecules were evenly distributed. The cell would then be cooled gradually (usually overnight) to its final working temperature.

Having measurements of temperature and pressure allowed us to calculate the chemical potential,

$$\mu(T,P)=k_B T \ln\left[\frac{1}{k_B}\left[\frac{2\pi\hbar^2}{mk_B}\right]^{3/2}\frac{P}{T^{5/2}}\right] + B(T)P+\mu_{\rm rot}(T)\ . \tag{1}$$

Here $B(T)$ is the second virial coefficient of methane gas,[17] and $\mu_{\rm rot}$ is a contribution from the rotational energy levels of the methane molecule.[18] Strictly speaking, this is the chemical potential of the vapor above the film, but since the film and the vapor are in equilibrium, their chemical potentials must be equal.

Temperatures, meanwhile, could be resolved to within about 2 mK. This meant, since temperature intervals on the order of 1 K were used, that absolute heat-capacity measurements were made with a precision of ±0.2%. However, the film accounted for, typically, 5–10% of this value, and when the cell's contribution was subtracted off, the scatter in the film heat-capacity measurements was correspondingly magnified. Furthermore, since these data were not isosteric, we had to correct for desorption. The heat of desorption is easily calculated if we know $(\partial\mu/\partial T)_N$,[19] N being the number in the film, but in a typical heat-capacity measurement N decreases so that the best we can hope for is $(\partial\mu/\partial T)_X$, where X denotes the experimental conditions. At low-enough temperatures (and hence vapor pressures) desorption is negligible so $(\partial\mu/\partial T)_N$ can be approximated by $(\partial\mu/\partial T)_X$. However in our case, this was not sufficient, so we had to rely on the *combined* vapor-pressure and heat-capacity data set to make this correction. Basically, we had measured μ on a dense T-N grid independently of the heat capacities (see the next section). Interpolating on this grid allowed us to compute $(\partial\mu/\partial T)_N$, and thus properly make the desorption correction. This correction was not negligible, and accounted for up to 50% of the film's contribution to the heat-capacity signal. Then, having true heat capacities on a similar (but less dense) T-N grid, we could interpolate to get true isosteric values.

The surface area of the substrate was measured by per-

forming a helium vapor-pressure isotherm at 4.2 K.[20] This yielded a $\frac{1}{3}$-ordering coverage of $N_{1/3}=77.3\pm0.3$ STPCC (standard temperature and pressure cubic centimeters corresponding to a surface area of 326 ± 1.4 m^2. Methane isotherms (see the next section) yielded a value of the coverage of 83.3 STPCC at the "knee" in the first-layer part of the measurement. This corresponded to Thomy and Duval's "V_{B1},"[21] and was used to match our data to theirs in the region where they overlap. (Because of methane's low vapor pressure and the enormous size of our substrate's area compared to theirs, the gas-distribution problems mentioned above prevented us from making reliable pressure measurements in the submonolayer regime). Later authors[22,23] have chosen to define one methane monolayer at an inflection point in the isotherm, i.e., at a coverage 9% greater than Thomy and Duval's V_{B1}. Defined in that way our own monolayer is 90.9 STPCC, and this correlates very well with our independently measured value of $N_{1/3}$, known to be about 85% of a monolayer.[22–24] Futher experimental details can be found in Ref. 13.

III. RESULTS

On the basis of our data, we wish to put forth two tentative conclusions concerning the behavior of methane multilayers on graphite. Both should be regarded in the spirit of hypotheses, suggested by preliminary survey data, and requiring further experimental verification by means of new, independent, and more detailed measurements.

The first of these is that the layer-by-layer critical temperature for condensation, $T_c(n)$, is roughly independent of n in the range $1\lesssim n\lesssim 6$, where n is the layer number, with $T_c(n)\approx 78$ K. (This sort of behavior, in fact, has been predicted by sophisticated treatments of the lattice-gas problem.[5–8]) If this result is extrapolated to large n, then in the context of the PSW model, it implies a roughening transition in bulk methane at about the same temperature.

The second is that the melting transition descends from bulk coexistence into the multilayer film region at essentially constant temperature, $T_m(N)\sim T_t$. The change in entropy associated with the transition declines smoothly, reaching zero at roughly two layers. It is not entirely clear how the transition closes. The transition does not appear to be first order in the multilayer region. In this section we shall discuss the data from which these conclusions have been drawn.

Figure 3 is a map showing the region surveyed in this study. Broadly speaking, there are data from nine heat-capacity runs extending from 65–100 K for films between 0.5 and 2.5 layers, and four runs between 4 and 6 layers, and vapor-pressure data from 78–96 K between 0.5 and 6 layers. To anchor this grid to zero coverage, we make use of adsorption isotherm data (on exfoliated graphite) by Thomy and Duval in the region 75–84 K, 0–1 layer, overlapping both our heat-capacity and vapor-pressure data.

The data upon which our analysis is based are shown in Figs. 4 and 5. In Fig. 4 we show the total heat capacity of the film. These are nonisosteric data, the coverage decreasing with increasing temperature. They must subsequently be interpolated to give isosteric values, or corrected by thermodynamic means to give, for example, the specific heat at constant spreading pressure, C_ϕ. Figure 5 shows vapor-pressure data displayed in the form N (coverage) versus μ (chemical potential). The plots are actually generated from computer outputs of straight-line segments connecting experimental points at the same temperature.

For orientation, Fig. 6 shows what appears to be the phase diagram of the first layer of methane on graphite, compiled from a variety of sources.[2–24] Note in particular that the gas-liquid critical temperature is believed to occur at approximately 75 K. If the first layer is the thin-film limit of our system, the opposite limiting case is bulk coexistence. On the bulk coexistence curve, there is a triple point separating solid and liquid phases at 90.7 K. Our isotherm data thus span a temperature region between $T_c(1)$, the first-layer critical point, and beyond T_t, the bulk triple point.

Evidence for the two principal conclusions we have tentatively put forth is easily seen in the raw data of Figs. 4 and 5. The most prominent feature of the heat-capacity curves is a sharp peak in the thicker films at $T_p\simeq 90$ K. The peak gets smaller as the film becomes thinner, but it does so at constant temperature, and there is still a vestige of it to be seen at about 2.5 layers. (A linear extrapolation of peak height versus coverage shows that it would disap-

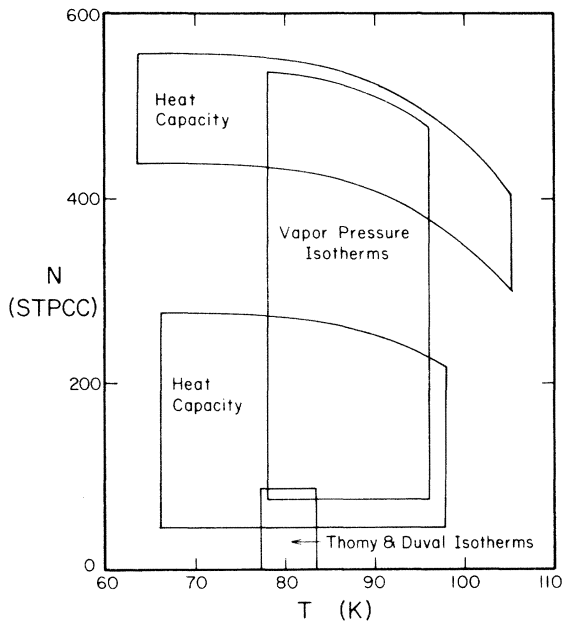

FIG. 3. Regions in the coverage-temperature plane where we have taken data. There are four runs in the upper heat-capacity block, and nine in the lower block with temperature intervals between points of roughly 1 K. Meanwhile, there are vapor-pressure isotherms at precisely spaced 1-K intervals from 78–96 K, running from just under 1 layer to between 5 and 6 layers. (One nominal monolayer is 90.9 STPCC). Furthermore, in order to bridge the gap from 0 to 1 monolayer, we have scaled Thomy and Duval's isotherms (see Ref. 21) to match with ours in the range of 77–84 K.

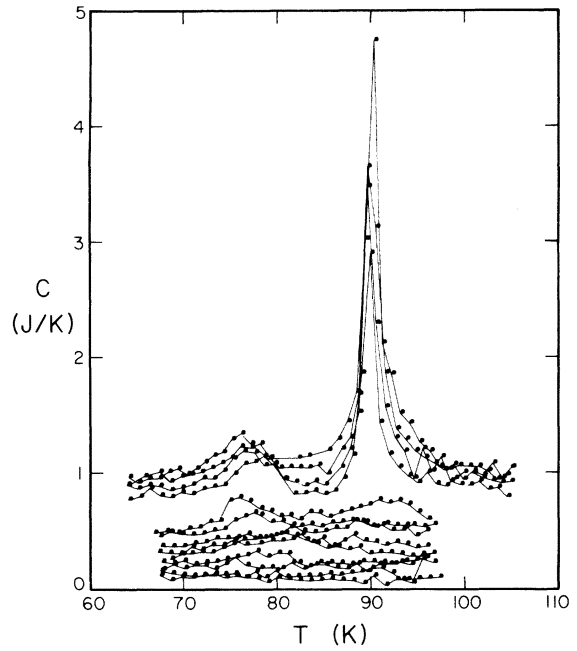

FIG. 4. Methane-film heat capacities for coverages ranging from 1.5 to 6 nominal monolayers. Although these data have been properly corrected for desorption (see text), they are not isosteric since the coverage decreases monotonically with temperature. The most prominent features are a very large peak near 90 K (close to the bulk triple temperature), and a smaller bump near 78 K. The large peak diminishes in size as the coverage is decreased, and disappears at about 2 layers. The significance of these features is discussed in the text.

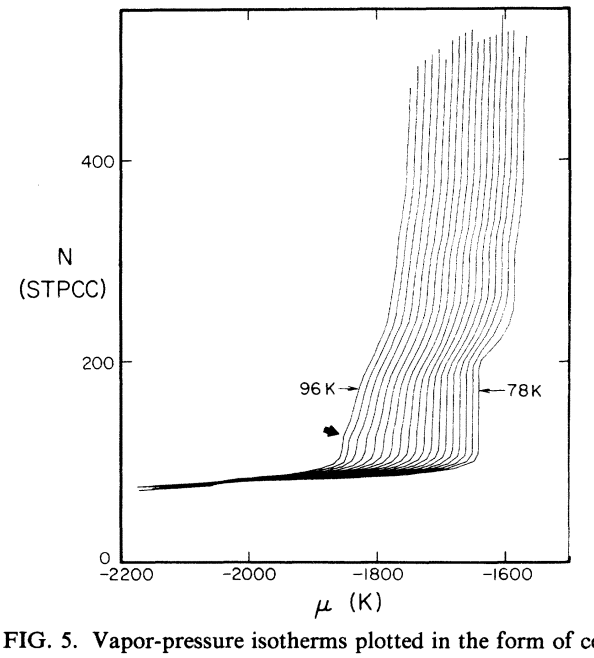

FIG. 5. Vapor-pressure isotherms plotted in the form of coverage vs chemical potential, at 1-K intervals from 78–96 K. The curves pass through some 750 experimental points whose symbols have been suppressed for the sake of clarity. Visible in these curves are the demarcation of distinct layers (up to about 5), and a possible phase transition in the second layer noted by the arrow. Furthermore, though unresolvable in this figure, details of the first-layer melting curve can be gleaned from these data.

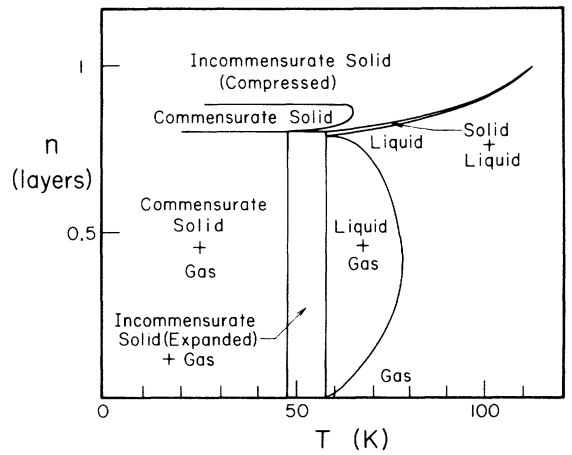

FIG. 6. Phase diagram for the first layer of methane adsorbed on graphite taken from a number of sources. (See Refs. 21–24.) Although details of this diagram might be subject to future reinterpretation, there is a 2D solid-liquid-gas triple point near 57 K, a 2D critical point near 75 K [corresponding to PSW's $T_c(1)$], a melting curve, and various commensurate-incommensurate solid-phase boundaries. (Note: It is not known how—or even if—the first-layer melting curve ends.)

pear entirely at about 2.1 layers.)

The heat capacity at bulk coexistence has a δ-function infinity at $T_t = 90.7$ K because at that point the system temperature does not change until the heat of fusion has been provided. It is natural to assume that the sharp peaks in Fig. 4 are remnants of this triple-point behavior, the area under the peak being associated with the entropy of melting. However, the peaks are clearly not δ functions, nor do they have the "mesalike" shape one would expect of essentially constant coverage heat capacities at a first-order phase transition in a thin film.[25]

Some years ago, a number of groups[26] carried out studies of the heat capacity of multilayer films near the bulk triple point in a variety of systems. The general trend of the results was that the bulk triple-point δ function became broadened and its maximum moved to lower temperature as the film became thinner. By contrast, in the present study, neither the width of the peak nor its temperature appears to change with film thickness. We believe this difference from the earlier studies to be due to the much greater uniformity of the graphite substrate we have used. The situation seems closely analogous to that of multilayer heat capacities for helium near the bulk λ transition: Bretz[27] reported heat-capacity anomalies of constant width and temperature (but declining height with film thickness) for helium on graphite near the temperature of the λ transition, whereas earlier studies on other substrates gave results strikingly similar to the early melting-point data we have cited above.[28]

On the other hand, our results are very similar to the multilayer heat capacities for nitrogen on graphite reported by Chung and Dash.[29] Chung and Dash interpreted the sharp peak they observed at the temperature of the bulk triple point to mean nonwetted films, the peak being contributed by the melting of beads of bulk matter. We are able to rule out that interpretation by means of the data in Fig. 5: The chemical potential is measurably

lower than the coexistence value for all of the data in this report. That means no beads of bulk matter can have formed.

Although beading, or nonwetting, can be ruled out as an explanation for the 90-K heat-capacity peaks, it is more difficult to rule out an alternative explanation, capillary condensation. Capillary condensation occurs when the effect of surface tension is to make it profitable to form bulk material in pores and cracks in the substrate before film growth is completed; negative curvature of the bulk matter-gas interface at the mouth of each pore allows coexistence at pressures below the bulk vapor pressure. The heat-capacity peaks we observe would then be due to the melting of bulk matter formed in this way.

The onset and extent of capillary condensation depends on the geometry of suitable imperfections in the substrate which, of course, is unknown. However, we may assume that capillary condensation begins to occur when the film thickness exceeds ~ 2 layers because that is where the 90-K peaks begin to appear. If we then analyze the entropy change associated with the peaks, we conclude that, in order to account for them, about half the matter adsorbed beyond the first two layers must be in capillary-condensed bulk form when the nominal coverage is 4.5 layers. (The melting entropy of the bulk is 1.24 k_B/molecule. The equivalent of more than a full layer in bulk form would have to melt to account for a peak the size of that in the 4.5 layer film).

The circumstantial evidence does not favor this view. Steps in adsorption isotherms, indicating layer-by-layer condensation, are approximately the same size up to at least the fifth layer in the methane-on-graphite system. This may be seen, with rather poor resolution in the thicker films, in our Fig. 9. It is seen more clearly in a 77-K isotherm by Thomy and Duval.[21] Capillary condensation to the extent necessary to explain our heat-capacity peaks is clearly inconsistent with their data in the fifth layer. To be sure, we have used a different substrate, but our uncompressed graphite foam should be at least as free of cracks and pores as the exfoliated graphite used by Thomy and Duval. Thus, although the evidence is not decisive, it is sufficient to lead us to choose against putting forth capillary condensation as the explanation for the behavior we observe at 90 K.

Our tentative conclusion, then, is that melting extends from the bulk triple point down to approximately 2 layers, at nearly constant temperature. We should point out that if the temperature is truly constant, the transition must be first order. A higher-order transition is one that occurs without a discontinuity in N. Thus, the condition for the phase boundary is

$$\mu_s(T,N)=\mu_l(T,N)\ ,$$

where $\mu_{s,l}$ are the chemical potentials of the lower- and higher-temperature phases. If we further specify that $T=T_t$, then there is a unique solution for N. Such a transition cannot occur for all N at the same temperature. This argument should be borne in mind in assessing our observation that melting occurs at nearly constant temperature, but does appear to be first order.

The obvious next question, then, is how does it close? Is there another phase boundary available for it to end on? Obvious candidates include the melting curve in the first layer (see Fig. 6), and whatever phase transition (melting for example) might be found in the second layer above $T_c(2)$.

Figure 7 shows some possible phase boundaries in the n-T plane. Bulk melting descends at nearly constant T, ending (or becoming undetectable) at about $n=2$. On the same scale we show first-layer melting, and a possible phase transition in the second layer.

In our vapor-pressure data, we observe a series of kinks in the second layer which could be interpreted as a phase boundary. The positions of these kinks are indicated by an arrow in Fig. 5, and their locus is plotted in Fig. 7. (They can perhaps be seen most easily, however, in Fig. 12.) If it is a phase transition, it could, for example, be the melting of the second layer. It occurs at roughly 1.33 layers, which seems rather a low density for second-layer melting to occur, but of course many kinds of transitions in thin films have been conjectured (orientational order-disorder, for example).

To conclude this discussion, we do not observe the extension of the bulk melting to close on a known transition. It seems to end rather far from first-layer melting. It is closer to, but not known to arrive at a possible transition

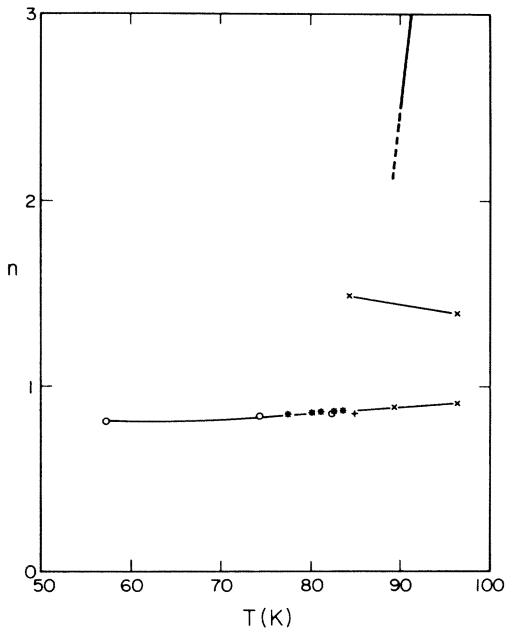

FIG. 7. Suggested phase boundaries in the range of one to three nominal monolayers. The vertical line near 90 K is a melting transition, we believe, and should extend upward to the bulk triple point. That being the case, there should be no path from the left of the line to the right which does *not* pass through some sort of boundary. We see no evidence for the extension of the line below 2 layers, so it either continues downward as a "thermodynamically invisible" transition, or links up in some unknown way with another phase boundary. The line in the middle marks the locus of points where we see a change in slope of the vapor-pressure isotherms. The lower line maps out the first-layer melting curve as reported in Refs. 21 (*), 23 (○), 24 (+), and this work (×).

of unknown nature in the second layer. An additional possibility is a thermodynamically undetectable melting transition of the type suggested by the Kosterlitz, Thouless, Halperin, Nelson, and Young (KTHNY) theory.[12]

Our second conclusion concerns $T_c(n)$. In the data of Fig. 5, one easily sees vertical, or very nearly vertical steps (N increasing at constant μ) in the second and third layers at 78 K, becoming distinctly less vertical at higher temperature. At the same time, there is a bump in each heat capacity, from ~ 2 to ~ 5 layers at about 78 K. We propose that this behavior results from a $T_c(n)$ at about that same temperature for n up to at least 5, and perhaps 6.

The heat-capacity bumps may be seen in Fig. 4. From about 3 layers up, they are about the same size in total heat capacity, suggesting they represent a phenomenon involving the same quantity of matter, i.e., the top layer. Bumps are present in the second layer, but they are smaller and more difficult to see on the scale of Fig. 4, while there is none detected in the first layer, where the data of many authors[21–24] clearly indicate one ought to be present. It would appear that substrate inhomogeneities, always important when the 2D compressibility is high, suppress the bump in the first layer, diminish them in the second layer, and have less effect at higher coverages.

The PSW model suggests that $T_c(n)$ will vary smoothly from $T_c(1)$ to T_R, the bulk roughening temperature as $n \to \infty$. One intriguing possibility is that T_c will increase with n, with, for example, $T_c(2) > T_c(1)$. In that case, at $T_c(2) > T > T_c(1)$, an adsorption isotherm of the type shown in Fig. 5 should be more vertical in the second (and higher) layers than in the first. This behavior would be somewhat counterintuitive, since one generally expects sharper features in the first layer than in higher layers.

To test this idea, we have combined our results with first-layer data by Thomy and Duval, using the proper substrate area scaling factor as mentioned in Sec. II. Isotherms constructed in this way for 78 K $\leq T \leq$ 84 K are shown in Fig. 8. (The Thomy and Duval data have been interpolated to match the temperatures of our survey grid.) One sees what appears to be the predicted behavior, with, for example, the second-layer steps being distinctly more vertical than the first.

However, the effect may be an artifact of the way in which the data are presented. The first layer occupies a much larger range of μ than does the second. This tends to stretch out the first-layer step, making it appear less vertical, and compress the second layer, making it appear more vertical.

To improve our view of the situation, we may plot the data in a different way, based on an excessively crude model of adsorption. The model is that $\mu(T,N)$ differs from the bulk coexistence value $\mu_0(T)$ only by the van der Waals potential of the substrate. In particular, if we take the van der Waals potential to be α/d^3 where α is a constant and d the film thickness, we have the Frenkel-Halsey-Hill isotherm,

$$\mu - \mu_0 = -\alpha/d^3 \,. \tag{2}$$

This model neglects precisely the interactions which give rise to the critical-point behavior we are examining. However, it does suggest that if we plot N vs $(\mu_0 - \mu)^{-1/3}$, we will be giving more nearly equal space on the graph to each layer.

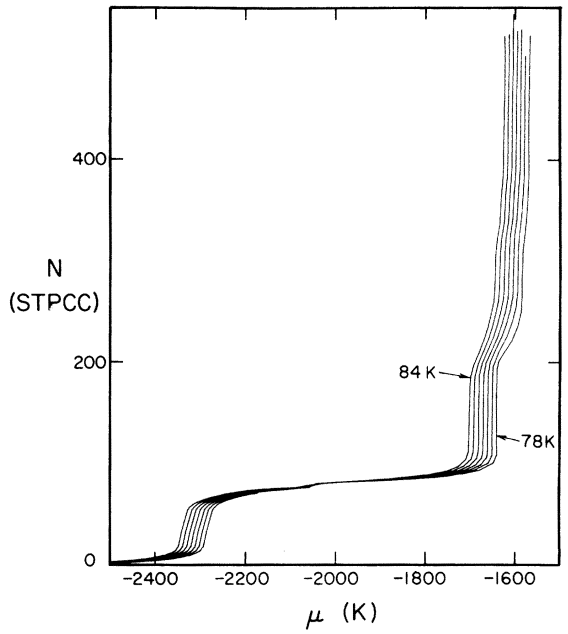

FIG. 8. Combined isotherms of this work and Thomy and Duval in the range of 78–84 K. The increased verticality of the second-layer step over the first lends credence to the idea that $T_c(2) > T_c(1)$. However, the horizontal scale expands first-layer details far out of proportion to the rest of the diagram, and so care must be taken to avoid drawing erroneous conclusions from this plot. A way of plotting the same data so that equal weight is given to each layer is shown in Fig. 9 below.

A plot of this kind is shown in Fig. 9 at $T = 80$ K. We see that the first three steps now appear about equally vertical. Evidence of a fourth step is also seen. The smearing out of the steps in higher layers is due to loss of experimental resolution as $\mu \to \mu_0$.

Analysis of experimental data to choose a precise $T_c(n)$ in each layer is extremely difficult. On an ideally homogeneous surface, a first-order phase transition at $T < T_c$ would show up as a truly vertical step on an isotherm. Thus, T_c would be the lowest temperature at which the isotherm has no vertical portion. However, as Dash and Puff have pointed out,[30] in a real system the substrate presents a distribution of binding energies. The condensed phase begins to form on the most strongly binding sites, and as condensation proceeds, the interface between high- and low-density phases sweeps through the distribution of binding energies of the substrate. Consequently, μ, rather than being constant during condensation at constant T, has a shape that reflects the distribution of site-binding energies. This effect is most clearly seen in data for ^{3}He (Ref. 31) and ^{4}He (Ref. 19) on Grafoil, where the 0-K isotherms, N vs μ, have been reconstructed thermodynamically. At low coverage, the $\sqrt{3}$ registered phase coexists with a two-dimensional vacuum (the two-dimensional vapor pressure is zero). In these cases, the 0-K isotherms are not quite vertical (i.e., μ changes as N is increased) and the results are used to deduce the distribution of binding ener-

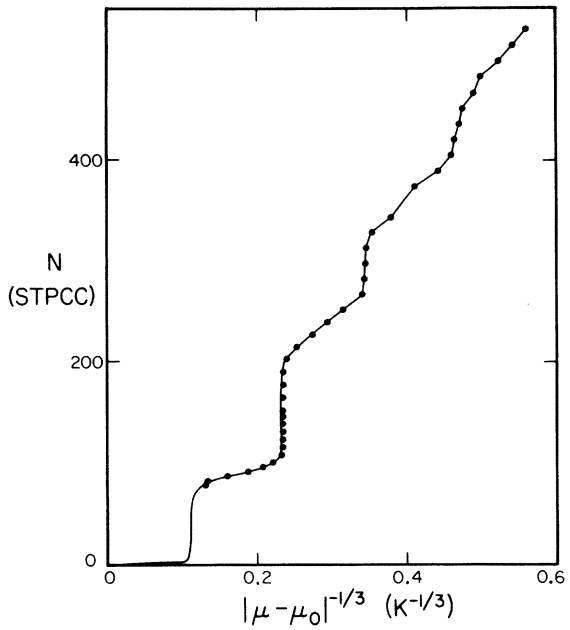

FIG. 9. Combined isotherm at 80 K plotted so as to give equal space to each layer. Now the verticality of the first three steps appears to be roughly the same. Note that this form of plotting magnifies the scatter in the upper layers. Our points are shown, whereas Thomy and Duval's are too numerous to stand out distinctly.

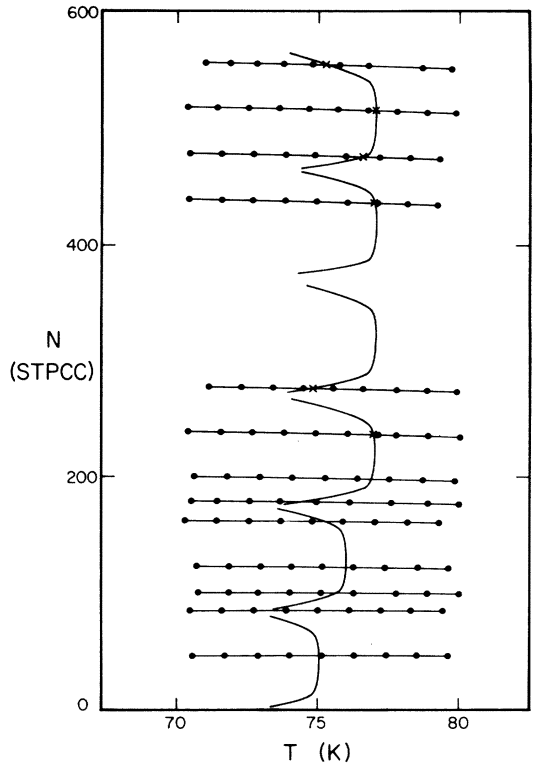

FIG. 10. Actual heat-capacity trajectories in the temperature range where the small bumps occur. If these bumps are to be interpreted as crossing from two-phase coexistence regions to single-phase regions, then the two-phase regions must end at $T_c(n)$'s of ~ 78 K, nearly independent of n. Moreover, the rounded ends of these regions must be fairly blunt, so that trajectories always cross them in the range of 76–78 K. (This behavior is similar to that shown in Fig. 5 of Ref. 7.) Only the six upper coverages show pronounced bumps, however.

gies. The important point for this study, however, is that even in a first-order coexistence region, isotherms are not expected to be vertical.

When the data plotted in Fig. (5) are examined in numerical form, it is found that the steps we observe are never quite vertical. That is to say, there is sufficient experimental resolution to show that $\mu(N_2)>\mu(N_1)$ whenever $N_2>N_1$. As we have just argued, that is necessary but not sufficient evidence to conclude that we are observing supercritical behavior at all N. In our view, the small bumps in the heat-capacity curves at $T\approx 78$ K are a better qualitative indication of the situation. We interpret them to mean that the shapes of the coexistence curves in each of the first 4 or 5 layers is such that one is very likely to pass out of the two-phase region at about 78 K.

If one passes out of a two-phase region along paths such as those sketched in Fig. 10, one expects a heat-capacity signal varying from a discontinuity (if the phase boundary is intercepted far from the critical point) to an Ising-type singularity (at the critical point). However, because the two-phase region is one of infinite (two-dimensional) compressibility, inhomogeneities in even the best real substrates may be expected to smear any of these heat-capacity signals into something that resembles the bumps we have in Fig. 4.[25] We thus propose that the bumps indicate a phase diagram of the kind sketched schematically in Fig. 10.

The arguments we have presented above constitute the case in favor of the two tentative conclusions we have put forth. We shall return in Sec. IV to discuss briefly some further implications of those conclusions. A complete thermodynamic analysis of our data will be presented elsewhere.[13] However, we shall conclude this section with a few quantitative details that seem relevant to our central points.

Figure 11 shows thermodynamically corrected specific heats at coverages of 430 and 232 STPCC. This figure makes it clear that whereas the peak at the triple-point temperature vanishes dramatically in thinner films, the smaller bump at 78 K is of essentially constant size in the specific heat. If we take the low-coverage curve in Fig. 11 as an indication of the background behavior not involved in the melting transition, we can subtract it off and use the remaining large peak to estimate the change in entropy. If we attribute that change to the amount adsorbed in excess of two layers, the result is $0.64k_B$/molecule compared to an entropy of melting of $1.24k_B$/molecule in bulk methane.

In Fig. 12, we have plotted all of our vapor pressure data in the form N vs $\mu-\mu_0$.[32] This has the effect of collapsing the data into a nearly universal curve. To put it differently, for many values of N, $\mu-\mu_0$ depends only on N, not T:

$$\mu-\mu_0=f(N)\ . \tag{3}$$

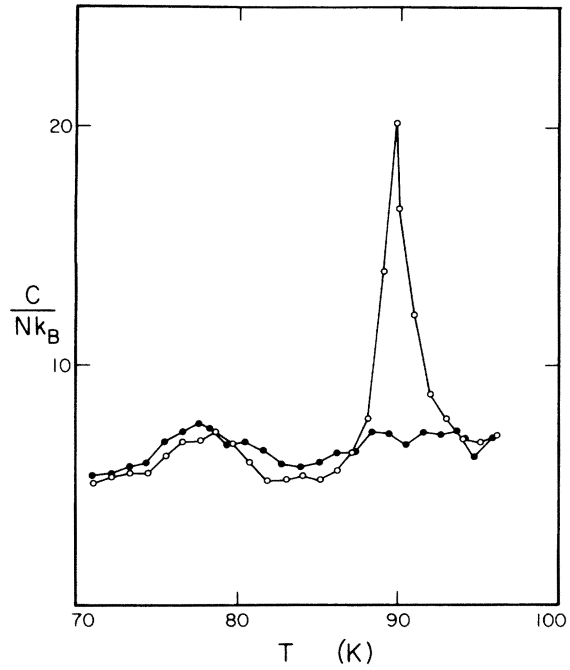

FIG. 11. Specific heats for films of two different thicknesses. The thicker-film (430 STPCC) data have been corrected to isostericity by interpolation, and show a pronounced melting peak. The thinner film (232 STPCC) does not show a melting peak, but retains the smaller bump at roughly 78 K.

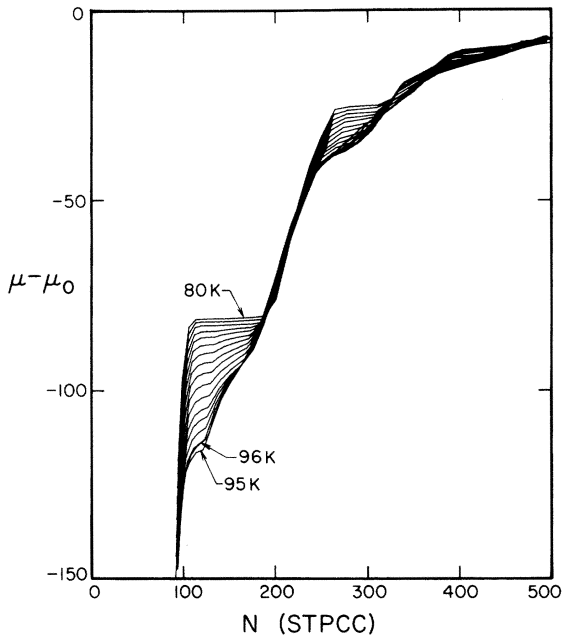

FIG. 12. Chemical potential (relative to the bulk) vs coverage for temperature between 80 and 96 K. In principle, whenever these isotherms coincide then the film is behaving like a slab of bulk. This notion is tested quantitatively in Fig. 13 below. Note that the films deviate most from bulk behavior in those regions where distinct layers make their presence felt. Note also the structure near 130 STPCC indicative of a possible phase transition in the second layer.

Equation (2) above suggests a particular model for $f(N)$. It is easy to show that a thermodynamic consequence of Eq. (3) is

$$\left[\frac{\partial S}{\partial N}\right]_T = s_b - v_b \frac{dP_0}{dt} , \tag{4}$$

where $(\partial S/\partial N)_T$ is the partial molar entropy of the film, and s_b is the specific entropy, v_b the specific volume, and P_0 the saturated vapor pressure of the bulk condensed phase at coexistence. To the extent that the second term on the right can be ignored (it is roughly 0.01% of the first), every molecule added to the film has the entropy of a molecule in the bulk. Thus, the coalescing of the isotherms in Fig. 12 means that the essential thermal behavior of the film is that of the bulk, and the curve that remains, $f(N)$, is indeed due to the van der Waals potential of the substrate.

There are, however, prominent regions in Fig. 12 where the isotherms do not coalesce. These are precisely the regions where the thermal behavior of the system is dominated by layer-by-layer condensation, which is characteristic of the thin-film nature of the system and not similar to the behavior of the bulk.

If Eq. (3) is not satisfied perfectly, in other words, if $f(N)$ does have some dependence on T, then the difference between $(\partial S/\partial N)_T$ and s_b is given by $(\partial f/\partial T)_N$. To examine the quantitative significance of the apparent coalescing of the curves in Fig. 12, we have computed $(\partial f/\partial T)_N$ from the numerical data at three coverages where the curves in Fig. 12 seem to coincide. The result is shown in Fig. 13. The scatter in this measurement is comparable to the change in entropy of the bulk when it melts. The significance of this observation is that the coalescing of the isotherms cannot be taken to mean that thin films are solidlike below T_t and liquidlike above. Measurements of $\mu(T,N)$ by means of vapor pressure are not sufficiently sensitive to detect that difference. On the other hand, it is precisely that difference that shows up as the very large spike in the heat capacity in the thicker films at T_t.

To summarize this discussion, layer-by-layer condensation is seen clearly in the data for $\mu(N,T)$, but only weakly in the heat capacity—it would not be possible to offer an interpretation of the small heat-capacity bumps at 78 K without guidance from the vapor-pressure data. Conversely, the effect of bulk melting are seen vividly in the heat-capacity data, but are essentially undetectable in $\mu(N,T)$. Both kinds of data are needed to survey the behavior of adsorbed systems.

IV. CONCLUSIONS

This study set out to survey methane multilayer films on graphite in the region between $T_c(1)$, the first layer critical temperature, and T_t, the bulk triple point. According to the PSW model, $T_c(1)$ should be the first in a series of transitions $T_c(n)$, with $T_c(\infty)=T_R$ the roughening transition, and T_t is the upper limit of possible roughening temperatures. Thus the survey could be expected to give interesting results, provided methane wets graphite in this temperature interval.

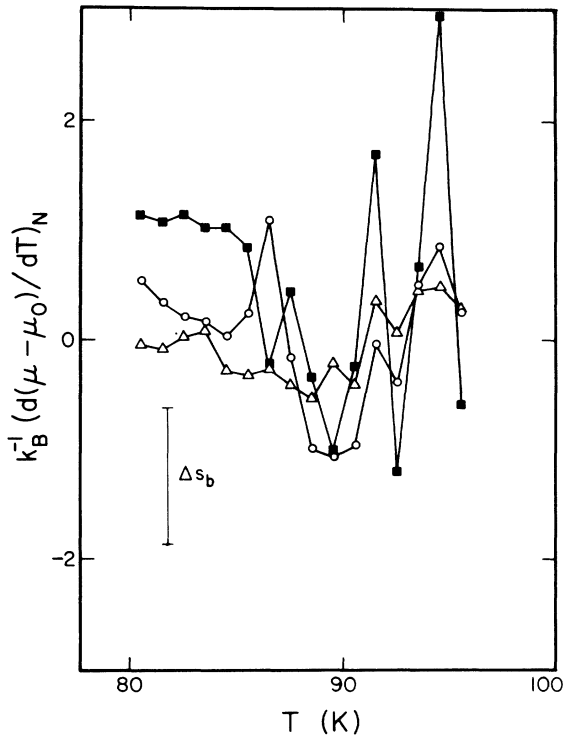

FIG. 13. The temperature derivative of $\mu-\mu_0$ at constant coverage vs temperature. These are finite-difference derivatives of unsmoothed data taken at three coverages where the curves of Fig. 12 coincide. The coverages are 371 (△), 218.5 (○), and 87.5 (■) STPCC. (Recall that one nominal monolayer is 90.9 STPCC.) In principle, $(\partial f/\partial T)_N$ measures the difference between the partial molar entropy of the film and the specific entropy of the bulk. However, the scatter in $(\partial f/\partial T)_N$ is comparable to the specific entropy of melting of the bulk, shown in the figure.

All of the data we have obtained are at $\mu<\mu_0$, that is to say, in a fully wetted film. Of course methane on graphite may have a finite wetting temperature T_W below the range we have studied (future measurements will investigate this point). It is also possible that methane begins to bead up in films of more than about 6 layers, but this seems exceedingly unlikely.

Beading up means that beads of bulk matter coexist with a uniformly adsorbed film. For this to occur, it is necessary that the film be in a state of higher intrinsic free energy than the bulk in order to balance its lower van der Waals potential. However, the evidence we have presented for methane on graphite is that a 5-layer film is so similar to the bulk that it melts at the same temperature. Thus the conditions necessary for beading up do not seem to be present.

We have presented evidence that there is a $T_c(n)\approx 78$ K independent of n for the first 5 or 6 layers. If we boldly extrapolate n from 6 to ∞, this implies a roughening transition at the interface between bulk solid methane and its vapor at $T\approx 78$ K.

The melting transition seems to extend from the bulk triple point into the multilayer region at essentially constant temperature. It does not appear to be first order in films of 5 layers and less. The entropy associated with melting (i.e., the area under the heat-capacity peak we associate with melting) becomes smaller as the film becomes thinner, vanishing altogether at about 2 layers. This effect does not appear to be due to capillary condensation.

The melting transition must close in some way because it should not be possible to follow any thermodynamic path from solid to liquid without passing through a phase transition. However, the data show only a phase transition that becomes successively weaker until it disappears into the experimental scatter. It does not appear to end on the first-layer melting curve, but there is some evidence of a phase transition of some kind in the second layer which might provide a way for the extension of the triple point to close. Alternatively it might end on a thermodynamically undetectable transition as suggested by KTHNY.

A complete thermodynamic analysis of the data presented here will appear elsewhere. The purpose of this paper has been to put forth hypotheses, suggested by these data and therefore requiring independent measurements, by thermodynamic and other techniques, to test them.

ACKNOWLEDGMENTS

We are grateful to Milton W. Cole, Joseph E. Avron, Michael Wortis, and Michael S. Pettersen for many stimulating and fruitful discussions. We would also like to thank André Thomy for sending us his data, and Michael B. Dowell of Union Carbide Corporation for providing us with noncommercial samples of Grafoil. This work was supported in part by a U. S. Department of Energy grant DE-AM03-76SF00767.

[1]R. Pandit, M. Schick, and M. Wortis, Phys. Rev. B 26, 5112 (1982).
[2]M. J. de Oliveira and R. B. Griffiths, Surf. Sci. 71, 687 (1978).
[3]R. Pandit and M. Wortis, Phys. Rev. B 25, 3226 (1982).
[4]C. Ebner, Phys. Rev. A 22, 2776 (1980).
[5]J. D. Weeks, Phys. Rev. B 26, 3998 (1982).
[6]C. Ebner, Phys. Rev. A 23, 1925 (1981).
[7]I. M. Kim and D. P. Landau, Surf. Sci. 110, 415 (1981).
[8]W. F. Saam, Surf. Sci. 125, 253 (1983).
[9]H. Nakanishi and M. E. Fisher, Phys. Rev. Lett. 49, 1565 (1982).
[10]In this picture $T_c(2)>T_c(1)$ because of a collective effect from the aggregate of adatoms. However, S. Rauber, J. R. Klein, and M. W. Cole [Phys. Rev. B 27, 1314 (1983)] have suggested another mechanism, namely that substrate screening weakens the attraction between adatoms in the first layer as compared to the second (and higher) layers.
[11]Reports of roughening transitions in other substances have

been put forth by J. E. Avron, L. S. Balfour, C. G. Kuper, J. Landau, S. G. Lipson, and L. S. Schulman Phys. Rev. Lett. 45, 814 (1980), and by K. A. Jackson and C. E. Miller, J. Crystal Growth 40, 169 (1977).

[12]The theory put forth by Kosterlitz, Thouless, Halperin, Nelson, and Young (hereafter referred to as KTHNY) is expounded in the following original papers: J. M. Kosterlitz and D. J. Thouless, J. Phys. C 6, 1181 (1973); D. R. Nelson and B. I. Halperin, Phys. Rev. B 19, 2457 (1979); A. P. Young, *ibid.* 19, 1855 (1979). See also W. F. Brinkman, D. S. Fisher, and D. E. Moncton, Science 217, 693 (1982).

[13]J. J. Hamilton, Ph.D. thesis, California Institute of Technology, 1983 (unpublished).

[14]L. G. Rubin and Y. Golahny, Rev. Sci. Instrum. 43, 1758 (1972).

[15]J. G. Dash and J. Siegwarth, Rev. Sci. Instrum. 34, 1276 (1963).

[16]T. Takaishi and Y. Sensui, Trans. Faraday Soc. 59, 2503 (1963).

[17]A series expansion for $B(T)$ based on a Lennard-Jones 6-12 intermolecular potential was used. See J. O. Hirschfelder, C. F. Curtiss, and R. B. Byrd, *Molecular Theory of Gases and Liquids* (Wiley, New York, 1964). The parameters used were $\sigma=3.187$ Å and $\epsilon/k_B=148.2$ K.

[18]L. D. Landau and E. M. Lifschitz, *Statistical Physics*, 3rd ed. (Pergamon, New York, 1980), Part 1. See p. 151. We have extended the partition function beyond the first few terms which they give. Moreover, ours is a factor of 16 larger (representing the nuclear spin degeneracy of four protons), since they calculate spin entropy as a separate quantity.

[19]R. L. Elgin and D. L. Goodstein, Phys. Rev. A 9, 2657 (1974).

[20]P. Taborek and D. Goodstein, Rev. Sci. Instrum. 50, 227 (1979).

[21]A. Thomy and X. Duval, J. Chim. Phys. 66, 1966 (1969); 67, 286 (1970); 67, 1101 (1970).

[22]P. Vora, S. K. Sinha, and R. K. Crawford, Phys. Rev. Lett. 43, 704 (1979). This is a neutron scattering study of which other examples are J. P. Coulomb, M. Bienfait, and P. Thorel, J. Phys. (Paris) Colloq. 38, C4-31 (1977), Phys. Rev. Lett. 42, 733 (1979); J. Phys. (Paris) 42, 293 (1981); M. Bienfait, Surf. Sci. 89, 13 (1979); A. Glachant, J. P. Coulomb, M. Bienfait, and J. G. Dash, J. Phys. (Paris) Lett. 40, L-543 (1979); M. W. Newberry, T. Rayment, M. V. Smalley, and R. K. Thomas, Chem. Phys. Lett. 59, 461 (1978), and G. Bomchil, A. Hüller, T. Rayment, S. J. Roser, M. V. Smalley, R. K. Thomas, and J. W. White, Philos. Trans. R. Soc. London, Ser. B 290, 537 (1980).

[23]J. H. Quateman and M. Bretz, Phys. Rev. Lett. 49, 1503 (1982).

[24]Y. Lahrer, J. Chem. Phys. 68, 2257 (1978).

[25]For a discussion of this point see R. E. Ecke and J. G. Dash (unpublished).

[26]See, for example, K. Dennis, E. L. Pace, and C. S. Baughman, J. Amer. Chem. Soc. 75, 3269 (1953); J. A. Morrison, L. E. Drain, and J. S. Dugdale, Can. J. Chem. 30, 890 (1952).

[27]M. Bretz, Phys. Rev. Lett. 31, 1447 (1973).

[28]Recently, however, these experiments have been reexamined, and somewhat different results were obtained. See J. Yuyama and T. Watanabe, J. Low Temp. Phys. 48, 331 (1982).

[29]T. T. Chung and J. G. Dash, J. Chem. Phys. 64, 1855 (1976).

[30]J. G. Dash and R. D. Puff, Phys. Rev. B 24, 295 (1981).

[31]R. L. Elgin, J. M. Greif, and D. L. Goodstein, Phys. Rev. Lett. 41, 1723 (1978).

[32]We obtain μ_0 from Eq. (1) by substituting the bulk saturated vapor pressure, P_0, for P. See G. T. Armstrong, F. G. Brickwedde, and R. B. Scott, J. Res. Natl. Bur. Stand. 55, 39 (1955) for values of P_0.